THE JOURNAL OF BIOLOGICAL CHEMISTRY VOL. 281, NO. 1, pp. 151–157, January 6, 2006
Printed in the U.S.A.

Subcellular Targeting and Differential *S*-Nitrosylation of Endothelial Nitric-oxide Synthase*

Received for publication, September 22, 2005, and in revised form, November 7, 2005 Published, JBC Papers in Press, November 14, 2005, DOI 10.1074/jbc.M510421200

Phillip A. Erwin[‡1], Douglas A. Mitchell[§2], Juliano Sartoretto[‡], Michael A. Marletta[§¶‖], and Thomas Michel[‡3]**

*From the [‡]Cardiovascular Division, Brigham and Women's Hospital, Harvard Medical School, Boston, Massachusetts 02115, the Departments of [§]Chemistry and of [¶]Molecular and Cell Biology, [‖]Division of Physical Biosciences, Lawrence Berkeley National Laboratory, University of California, Berkeley, California 94720, and the **Veterans Affairs Boston Healthcare System, West Roxbury, Massachusetts 02132*

Endothelial nitric-oxide synthase (eNOS) undergoes a complex pattern of post-translational modifications that regulate its activity. We have recently reported that eNOS is constitutively *S*-nitrosylated in endothelial cells and that agonists promote eNOS denitrosylation concomitant with enzyme activation (Erwin, P. A., Lin, A. J., Golan, D. E., and Michel, T. (2005), *J. Biol. Chem.* 280, 19888–19894). In the present studies, we use mass spectrometry to confirm that the zinc-tetrathiolate cysteines of eNOS are *S*-nitrosylated. eNOS targeting to the plasma membrane is necessary for enzyme *S*-nitrosylation, and we report that translocation between cellular compartments is necessary for dynamic eNOS *S*-nitrosylation. We transfected cells with cDNA encoding wild-type eNOS, which is membrane-targeted, or with acylation-deficient mutant eNOS (Myr^-), which is expressed solely in the cytosol. While wild-type eNOS is robustly *S*-nitrosylated, we found that *S*-nitrosylation of the Myr^- eNOS mutant is nearly abolished. When we transfected cells with a fusion protein in which Myr^- eNOS is ligated to the CD8-transmembrane domain (CD8-Myr^-), we found that CD8-Myr^- eNOS, which does not undergo dynamic subcellular translocation, is hypernitrosylated relative to wild-type eNOS. Furthermore, we found that when endothelial cells transfected with wild-type or CD8-Myr^- eNOS are stimulated with eNOS agonist, only wild-type eNOS is denitrosylated; CD8-Myr^- eNOS *S*-nitrosylation is unchanged. These findings indicate that subcellular targeting is a critical determinant of eNOS *S*-nitrosylation. Finally, we show that eNOS *S*-nitrosylation can be detected in intact arterial preparations from mouse and that eNOS *S*-nitrosylation is a dynamic agonist-modulated process in intact blood vessels. These studies suggest that receptor-regulated eNOS *S*-nitrosylation may represent an important determinant of NO-dependent signaling in the vascular wall.

The endothelial isoform of nitric-oxide synthase (eNOS)[4] is central to diverse cardiovascular homeostatic pathways including vasodilation, angiogenesis, and regulation of platelet aggregation (reviewed in Ref. 1). A constitutive enzyme, eNOS is robustly expressed by vascular endothelial cells and undergoes dynamic subcellular targeting that affects eNOS activity by differentially exposing the enzyme to diverse regulatory interactions, including enzyme inhibition by caveolin or activation by different kinases and phosphatases (2, 3). In resting cells, eNOS is targeted to caveolae by reversible thiopalmitoylation of eNOS Cys^{15} and Cys^{26}, modifications that are dependent on the prior co-translational and irreversible *N*-myristoylation of eNOS Gly^2 (4). Upon agonist stimulation, eNOS is rapidly depalmitoylated and translocates from peripheral membrane caveolae to internal membrane structures; over time, the enzyme is retargeted to caveolae and repalmitoylated as eNOS returns to basal activity levels (2, 5, 6). We have previously reported that *S*-nitrosylation reversibly inhibits eNOS activity, that eNOS is tonically *S*-nitrosylated in vascular endothelial cells, and that the enzyme undergoes rapid, transient denitrosylation upon agonist stimulation, followed by progressive renitrosylation as the enzyme returns to resting activity levels (7). We also showed that endogenous eNOS *S*-nitrosylation in transfected cells is abolished when the zinc-tetrathiolate cysteines (residues 96 and 101 in the bovine eNOS sequence) of eNOS are changed to serine by PCR-directed mutagenesis (7). We used mass spectrometry to analyze the *S*-nitrosylation pattern of purified recombinant eNOS and showed directly that the zinc-tetrathiolate of eNOS is preferentially *S*-nitrosylated in the intact enzyme. We also report that subcellular targeting is a determinant of eNOS *S*-nitrosylation and that translocation between cellular compartments is necessary for agonist-modulated eNOS denitrosylation. Finally, we extended our work from cultured bovine aortic endothelial cells (BAEC) to show that dynamic *S*-nitrosylation occurs in intact mouse blood vessels. Taken together, these data suggest that *S*-nitrosylation is a dynamic and physiologically relevant regulator of NO signaling pathways in the vascular endothelium.

EXPERIMENTAL PROCEDURES

Materials—Fetal bovine serum was from Hyclone (Logan, UT); all other cell culture reagents were from Invitrogen. Anti-eNOS monoclonal antibody was from Transduction Laboratories (Lexington, KY). Anti-phospho-eNOS-Ser^{1179} (Ser^{1177} in the human eNOS sequence) and anti-phospho-Akt-Ser^{473} antibodies were from Cell Signaling Technologies (Beverly, MA). Anti-HA monoclonal antibody 12CA5 used for immunoprecipitation of HA epitope-tagged eNOS was from Roche Applied Science. Anti-HA monoclonal antibody for immunoblot was from Santa Cruz Biotechnology (Santa Cruz, CA). Super Signal West Pico and Femto substrate for chemiluminescence detection, biotin-HPDP, and horseradish peroxidase (HRP) conjugated to secondary antibodies or to NeutrAvidin (NeutrAvidin-HRP) were from Pierce. VEGF was from Calbiochem. Wild-type C57BL/6J mice and mice in

* This work was supported by National Institutes of Health Grants HL46457 and HL48743 (to T. M.) and by grants from the DeBenedictis Fund of the University of California at Berkeley (to M. A. M.). The costs of publication of this article were defrayed in part by the payment of page charges. This article must therefore be hereby marked "*advertisement*" in accordance with 18 U.S.C. Section 1734 solely to indicate this fact.
[1] Supported by a Howard Hughes Medical Institute Predoctoral Fellowship.
[2] Supported by an American Heart Association Predoctoral Fellowship.
[3] To whom correspondence should be addressed: Cardiovascular Division, Brigham and Women's Hospital, Thorn Bldg. 1210A, 75 Francis St., Boston, MA 02115. Tel.: 617-732-7376; Fax: 617-732-5132; E-mail: tmichel@research.bwh.harvard.edu.
[4] The abbreviations used are: eNOS, endothelial nitric-oxide synthase; HA, hemagglutinin; biotin-HPDP, N-[6-(biotinamido)hexyl]-3′-(2′-pyridyldithio)propionamide; HRP, horseradish peroxidase; VEGF, vascular endothelial growth factor; DEA/NO, (*Z*)-1-(*N*,*N*-diethylamino)diazenium-1,2-diolate; MMTS, methyl methanethiosulfonate; MALDI, matrix-assisted laser desorption ionization; MS, mass spectrometry; CID, collision-induced dissociation; BAEC, bovine aortic endothelial cells; DMEM, Dulbecco's modified Eagle's medium; ANOVA, analysis of variance.

which the eNOS gene is disrupted (B6.129P2-Nos3$^{tm1/Unc/J}$) were purchased from Jackson Laboratories (Bar Harbor, ME). Protein A-agarose, anti-β-actin monoclonal antibody, and all other reagents were from Sigma.

Expression and Purification of Recombinant eNOS—Plasmid pCW-eNOS, encoding the cDNA of bovine eNOS (8) with an N-terminal hexahistidine tag, was obtained from Paul Ortiz de Montellano (University of California at San Francisco) (9). pCW-eNOS was transformed into competent BL21 (DE3) pLysS cells under selection with 50 μg/ml carbenicillin and 35 μg/ml chloramphenicol. A starter culture (30 ml) was grown overnight and used to inoculate 6 × 1-liter flasks of terrific broth. Cultures were grown at 37 °C to an A_{600} of ~0.8. The temperature was then lowered to 22 °C and recombinant eNOS expression was induced with 1.5 mM isopropyl β-D-thiogalactopyranoside for 18 h. Cells were pelleted by centrifugation and stored at −80 °C until purification. Cell pellets were resuspended in 4 °C lysis buffer (50 mM Na_2HPO_4, 300 mM NaCl, 10 mM imidazole, 10% glycerol, EDTA-free Complete Protease Inhibitor Mixture Tablets (Roche Applied Science), pH 8.0. The resuspended cells were lysed by sonication and further disrupted using an EmulsiFlex-C5 high-pressure homogenizer (Avestin, Ottawa, Canada) at 4 °C. Centrifugation for 1 h at 42,000 rpm yielded supernatant that was immediately gravity-loaded onto a nickel-nitrilotriacetic acid Superflow column (Qiagen). After loading, the column was washed with 20 volumes of wash buffer (50 mM Na_2HPO_4, 500 mM NaCl, 20 mM imidazole, 10% glycerol, pH 8.0), followed by 10 volumes of elution buffer (50 mM Na_2HPO_4, 500 mM NaCl, 250 mM imidazole, 10% glycerol, pH 8.0). Fractions containing full-length eNOS (~135 kDa), as determined by Coomassie-staining of samples separated by SDS-PAGE, were pooled and concentrated using 50-kDa molecular weight cut-off Vivaspin concentrators (Vivascience, Hannover, Germany). eNOS was further purified using a Superdex 200 HiLoad 26/60 gel filtration column (Amersham Biosciences) equilibrated with 100 mM HEPES, 100 mM NaCl, 500 μM L-arginine, 10 μM (*6R*)-5,6,7,8-tetrahydro-L-biopterin, and 10% (v/v) glycerol, pH 7.4. Fractions containing homogeneous full-length eNOS were pooled, concentrated, and stored at −80 °C. Deviation from these conditions or failure to keep eNOS at 4 °C or lower throughout the purification resulted in extensive proteolysis. Protein concentrations were assessed using the Bradford method (bovine serum albumin standard); the eNOS protein yield typically was 4 mg/liter.

Biotin Switch Method for Purified Recombinant eNOS—The biotin switch method was performed as described previously (10), with minor modifications outlined below. Initial protein concentration was 0.5 μg/μl, and reactions were performed in 125 μl total volume. For the first step of the assay, metal chelators were omitted to avoid disrupting the zinc-tetrathiolate cluster in eNOS. The buffer for the rest of the assay was 100 mM HEPES, 400 μM EDTA, and 40 μM neocuproine, pH 7.5. The presence of EDTA and neocuproine ensured that metal-catalyzed *S*-nitrosothiol decomposition would be minimized. Purified proteins were *S*-nitrosylated *in vitro* using the NO-donor diethylammonium (*Z*)-1-(*N*,*N*-diethylamino)diazenium-1,2-diolate (DEA/NO, 50 μM). The blocking step was performed at 55 °C, in the presence of 30 mM methyl methanethiosulfonate (MMTS) with frequent vortexing. Samples were then biotinylated, separated by non-reducing SDS-PAGE (10–20% Tris-glycine) and transferred to nitrocellulose membranes. Membranes were blocked overnight in 3% bovine serum albumin and probed in Western blots with NeutrAvidin-HRP. The Western blots were developed using Super Signal West Femto chemiluminescence reagent and the biotinylation signal for *S*-nitrosylation visualized on a Fluor-S Multimager (Bio-Rad).

Proteolytic Digests and MALDI-MS Analysis of Peptide Fragments—Purified recombinant eNOS (~15 μg) processed by the biotin switch method was diluted to a total volume of 35 μl in 50 mM ammonium bicarbonate, pH 7.8, and 5% v/v *n*-propyl alcohol. Omission of *n*-propyl alcohol from the digest reaction or starting with incompletely denatured eNOS both resulted in extremely poor proteolysis. Digestions were initiated with the addition of 180 ng of Trypsin Gold (Promega, Madison, WI) and incubated for 12 h at 22 °C. Samples for MALDI-MS were desalted using C-18 ZipTips (Millipore, Bedford, MA) and were eluted with 6 μl of a 60% acetonitrile, 39.9% H_2O, 0.1% trifluoroacetic acid solution saturated with α-cyano-4-hydroxycinnamic acid. The matrix/peptide solution (1 μl) was then spotted onto the MALDI target. Spectra were acquired in reflector mode over the range *m*/*z* 600–5000 Da using an Applied Biosystems Voyager-DE PRO mass spectrometer (Foster City, CA). To acquire collision-induced dissociation (CID) spectra, a single time-of-flight spectrum was first recorded on an Applied Biosystems 4700 MALDI tandem time-of-flight instrument in reflector mode over the range *m*/*z* 600–4500 Da. The protonated peptide ions at *m*/*z* 1003.4 and 1385.7 Da were then isolated in MS1 and individual CID spectra acquired. Air was used as the collision gas at 1.0 keV (laboratory frame) collision energy.

Cell Culture and Drug Treatment—BAEC were obtained from Cambrex (Walkersville, MD) and maintained in culture on gelatin-coated 100-mm culture dishes with Dulbecco's modified Eagle's medium (DMEM) supplemented with fetal bovine serum (10% v/v) and penicillin-streptomycin (2%). Experiments were performed with BAEC between passages 5 and 8; cultures were serum-starved overnight before experiments, and drug treatments of BAEC were performed as described (11). COS-7 cells were obtained from ATCC (Manassas, VA) and maintained on uncoated culture dishes in the same medium as BAEC (12). For stimulation with A23187, transfected COS-7 cells were equilibrated in Hanks' balanced salt solution with Ca^{2+} (1.26 mM) for 20 min at 37 °C. A23187 prepared in dimethyl sulfoxide (Me_2SO) was then added (final A23187 concentration of 10 μM), and the cells were incubated for a further 5 min at 37 °C. Me_2SO alone (final concentration 0.1%) was added to the control samples.

Plasmid Transfection—The plasmid pkENH encoding HA epitope-tagged wild-type bovine eNOS cDNA and its parent plasmid pBKCMV (Stratagene, La Jolla, CA) have been described previously (5). Plasmids encoding the *N*-myristoylation-deficient eNOS mutant (Myr^-) and the fusion protein in which Myr^- is ligated to the CD8-transmembrane domain have been characterized in detail previously (3, 13). BAEC and COS-7 cells were transfected with plasmids using FuGENE 6 (Roche Applied Science) according to the manufacturer's protocol.

Preparation of Cellular Lysates, Immunoprecipitation, and Biotin Switch Method for Detection of S-Nitrosylated eNOS—100-mm dishes of cells were washed with ice-cold phosphate-buffered saline and harvested by scraping into 1 ml of lysis buffer comprised of Tris (20 mM, pH 7.4), Nonidet P-40 (1% v/v), deoxycholate (2.5% w/v), NaCl (150 mM), Na_3VO_4 (2 mM), EDTA (1 mM), NaF (1 mM), and neocuproine (100 μM), supplemented with a mixture of protease inhibitors, as described previously (7). After vigorous vortexing, cellular lysates were sonicated on ice (Branson Ultrasonic, Danbury, CT) at 30% of nominal converter amplitude for 3 × 10 s bursts. Lysates were then rocked at 4 °C for 30 min and centrifuged at 14,000 × *g* for 15 min. eNOS was immunoprecipitated from COS-7 cells by incubating supernatants with anti-eNOS monoclonal antibody or from BAEC with anti-HA monoclonal antibody 12CA5. All antibody incubations were rocked for 1–16 h at 4 °C. After addition of Protein A-agarose beads and another hour of rocking at 4 °C, the beads were washed extensively with ice-cold lysis buffer. eNOS was then eluted by rocking the beads with "Blocking Buffer" (14) for 25 min

at room temperature before proceeding with blocking and biotinylation steps of the biotin switch method, essentially as described (7, 14). After the biotinylation step, labeled eNOS was purified with streptavidin-agarose, eluted by boiling in SDS-sample buffer, separated by SDS-PAGE under reducing conditions, and transferred to nitrocellulose membranes for immunoblot against eNOS, as described (7). Low light conditions were used until completion of the biotinylation step.

Analyses in Intact Blood Vessels—Mice were sacrificed with a lethal dose of Nembutol and the thoracic aortae promptly harvested following thoracotomy. Whole mouse aortae were immediately placed into ice-cold homogenizing buffer comprised of Tris (10 mM, pH 7.4), Triton X-100 (1% v/v), deoxycholate (0.5% w/v), SDS (0.1% v/v), NaCl (150 mM), Na_3VO_4 (2 mM), NaF (1 mM), and neocuproine (100 μM), supplemented with a mixture of protease inhibitors. After freezing on dry ice, samples were homogenized with a PowerGen 125 homogenizer (Fisher). Homogenate solutions were centrifuged at 14,000 × *g* for 2 min and rocked for 30 min 4 °C. After another 30 min of centrifugation at 14,000 × *g*, the supernatants were incubated with anti-eNOS antibody for 1–16 h at 4 °C, followed by incubation with Protein A-agarose beads for 1 h. eNOS was eluted from the beads into Blocking Buffer, processed by the biotin switch method, and separated by SDS-PAGE essentially as described above for eNOS prepared from BAEC above (7, 14). For VEGF treatments, freshly isolated aortae were first equilibrated in DMEM for 1.5 h at 37 °C. The medium was then exchanged for an equal volume of DMEM containing VEGF or its vehicle. After incubating in the new medium for 5 min at 37 °C, vessels were washed with DMEM and frozen in buffer for homogenization, eNOS immunoprecipitation, and processing by the biotin switch method, as described above.

Reduction of eNOS S-Nitrosothiols with $HgCl_2$—Following eNOS immunoprecipitation with anti-eNOS antibody and Protein A-agarose, eNOS was eluted by rocking the beads for 25 min at room temperature in a solution comprised of $HgCl_2$ (3 mM), HEPES (250 mM, pH 7.7), neocuproine (100 μM), and SDS (2.5%). The same solution without $HgCl_2$ was used for the control sample. The beads were pelleted by centrifugation and the supernatant reacted at 40 °C for 30 min with shaking and frequent vortexing. eNOS was precipitated with 1 volume of −20 °C acetone, incubated at −80 °C for 15 min, rocked at 4 °C for 20 min, and centrifuged for 30 min at 14,000 × *g*. The pellet was resuspended in Blocking Buffer and processed by the biotin switch method, as described (7).

Immunoblotting—After separation by SDS-PAGE, proteins were electroblotted onto nitrocellulose membranes and probed with antibodies as described, except that Western blots of mouse eNOS were probed with a 1:1000 dilution of anti-eNOS antibody (11). Immunoblots were probed for β-actin according to the manufacture's protocol. Immunoblots were stripped for re-blotting with ReBlot Antibody Stripping Solution from Chemicon International (Temecula, CA). Densitometric analyses of autoradiographs were performed using a Chemi-Imager 400 (Alpha Innotech, San Leandro, CA).

Other Methods—Mean values for individual experiments are plotted ± S.E. Data plotting and statistical analyses (ANOVA) were performed using Origin software (OriginLab, Northampton, MA). A p value less than 0.05 was considered statistically significant.

RESULTS

MALDI Mass Spectrometric Analysis of S-Nitrosylated eNOS—We used the "biotin switch" method to selectively and quantitatively label the *S*-nitrosylated cysteine(s) of eNOS for identification by mass spectrometry (15). In the biotin switch method, unmodified cysteine sulfhydryls of a protein are first reacted with MMTS, protecting them from biotinylation in the subsequent labeling steps and thereby preventing false-positive signals (14). Next, any cysteine *S*-nitrosothiols are reduced with ascorbate and reacted with a biotin-HPDP label (14).

Our first step was to use the biotin switch method to analyze *S*-nitrosylation of purified recombinant eNOS incubated with the NO-donor DEA/NO (50 μM). After processing by the biotin switch method, eNOS was subjected to non-reducing SDS-PAGE and transferred to nitrocellulose membranes. Probing the membranes with NeutrAvidin-HRP revealed a robust increase in the *S*-nitrosylation signal of purified recombinant eNOS treated with DEA/NO (data not shown). When we trypsinized DEA/NO-treated eNOS and analyzed the tryptic peptides by MALDI-MS, we detected peaks at 1003.4 and 1385.7 Da, which correspond to the peptide ^{101}CLGSLVLPR^{109} modified at Cys^{101} by MMTS and biotin-HPDP, respectively (Fig. 1). This peptide contains a non-tryptic N terminus and a tryptic C terminus. Please note that in Figs. 1 and 2, because of the N-terminal His_6-tag on the recombinant eNOS, the numbering of residues reflects the addition of these additional 6 histidine residues at the N terminus; thus Cys^{107} shown in the figure is equivalent to Cys^{101} in the bovine eNOS sequence. CID spectra derived from the 1003.4- and 1385.7-Da peptides (Fig. 2) confirm biotinylation of the C-terminal cysteine of zinc-tetrathiolate of eNOS, *i.e.* that Cys^{101} is *S*-nitrosylated. Despite extensive efforts using different proteases, matrices, and spotting techniques, we were unable to detect any peptide containing the free, MMTS- or biotin-adducted N-terminal cysteine of eNOS's zinc-tetrathiolate (Cys^{96}), a residue that we previously identified using site-directed mutagenesis as a site that undergoes *S*-nitrosylation (7).

eNOS Subcellular Targeting and S-Nitrosylation—We have previously reported that an acylation-deficient eNOS mutant (Myr$^-$), which is expressed solely in the cellular cytosol, is not *S*-nitrosylated (7). Because eNOS subcellular targeting is a determinant of eNOS's phosphorylation pattern (3), we proposed that eNOS *S*-nitrosylation may also influenced by subcellular targeting. To further explore this hypothesis, we transfected COS-7 cells with cDNA encoding recombinant wild-type eNOS, which reversibly transits between plasmalemmal caveolae and internal membranes; Myr$^-$ eNOS, which is expressed solely in the cellular cytosol; or with a fusion protein in which Myr$^-$ eNOS is ligated to the transmembrane domain of the cell surface glycoprotein CD8 (CD8-Myr$^-$) (3). We have previously shown that while the CD8-Myr$^-$ eNOS fusion protein is irreversibly targeted to plasmalemmal caveolae, this construct remains enzymatically active and can be stimulated by eNOS agonists (16, 17). Consistent with our previous findings (7), we found that wild-type recombinant eNOS immunoprecipitated from lysates of COS-7 cells and processed by the biotin switch method produces a robust *S*-nitrosylation signal (Fig. 3). By contrast, *S*-nitrosylation of the cytosolic Myr$^-$ eNOS mutant in transfected COS-7 cells is almost undetectable (15 ± 11% of wild-type signal, $n = 3$, $p < 0.05$) (7). Finally, the *S*-nitrosylation signal for the immunoprecipitated CD8-Myr$^-$ fusion protein is greater than that of wild-type eNOS (435 ± 150% of wild-type signal, $n = 3$, $p < 0.05$; Fig. 3).

Agonist-modulated eNOS Translocation and S-Nitrosylation—eNOS is tonically *S*-nitrosylated in resting endothelial cells (7). Upon agonist stimulation, eNOS is depalmitoylated and translocates from caveolae to internal membrane structures (6), a process that is temporally associated with enzyme denitrosylation (7). Based on our finding that differentially acylated eNOS constructs are differentially *S*-nitrosylated (Fig. 3), we hypothesized that dynamic eNOS *S*-nitrosylation may be intrinsically linked to eNOS subcellular translocation. To test this hypothesis, we examined the effect of VEGF, a potent eNOS agonist, on the *S*-nitrosylation patterns of recombinant wild-

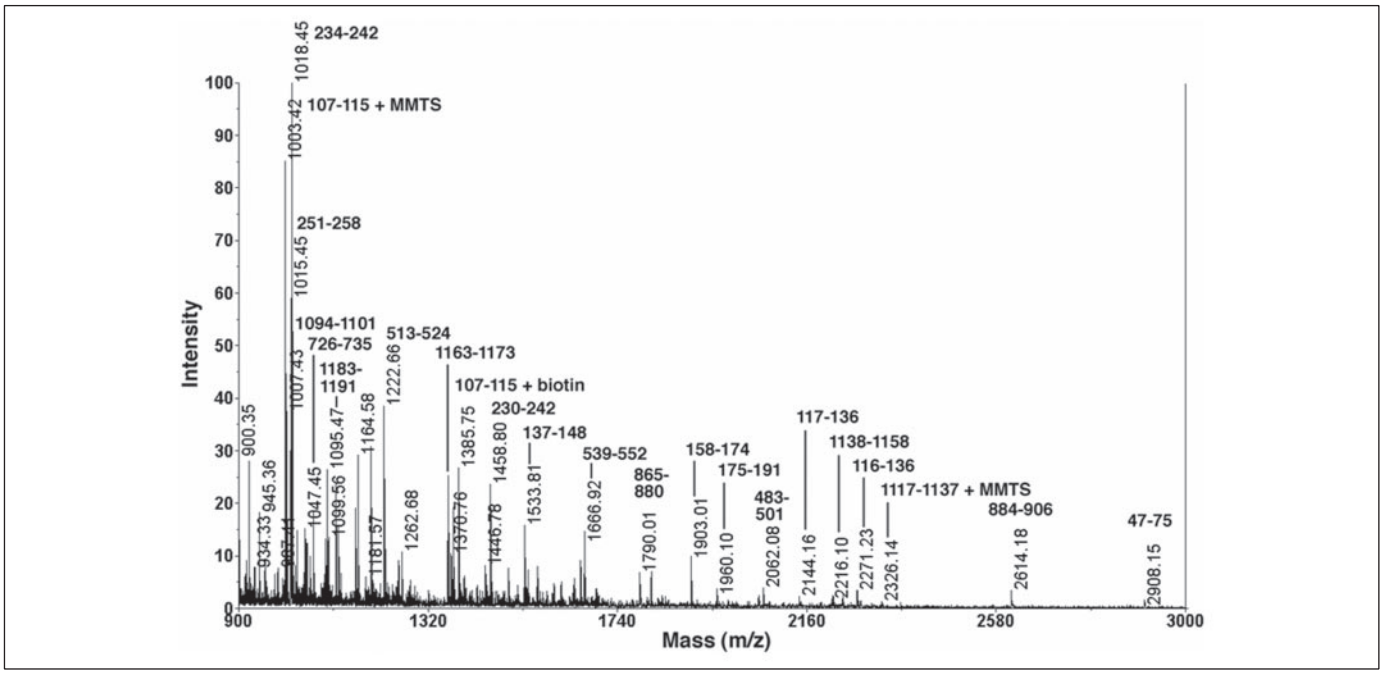

FIGURE 1. **MALDI-MS spectrum of tryptic peptides derived from eNOS processed by the biotin switch method.** Shown is a MALDI-MS spectrum derived from a 15-μg sample of recombinant purified eNOS processed by the biotin switch method and digested with 1:80 trypsin for 12 h at 22 °C, as described under "Experimental Procedures." After desalting on C-18 ZipTips, samples were co-spotted on the MALDI target with α-cyano-4-hydroxycinnamic acid, and a mass spectrum from *m/z* 600–5000 Da was acquired. For clarity, the range *m/z* 900–3000 Da is shown. No peptides above 3000 Da were detected. The N terminus of peptide 107–115 (corresponding to bovine eNOS 101–109) is the result of non-tryptic proteolysis. Numbering for the peptide assignments in this figure includes the N-terminal His_6-tag.

type eNOS or CD8-Myr^- eNOS in transfected BAEC (18). Both recombinant proteins are tagged with the HA-epitope and can be isolated from endogenous eNOS by immunoprecipitation with anti-HA antibody. As shown in Fig. 4*A*, both wild-type and CD8-Myr^- eNOS are *S*-nitrosylated in resting BAEC. In agreement with our previous studies, addition of VEGF (10 ng/ml for 5 min) acutely decreases *S*-nitrosylation of recombinant wild-type eNOS by 69 ± 4% compared with vehicle-treated BAEC ($n = 3$, $p < 0.001$ by ANOVA) (7). By contrast, we found that *S*-nitrosylation levels of CD8-Myr^- eNOS are not significantly affected by addition of VEGF (Fig. 4*A*). To explore whether agonist-modulated eNOS denitrosylation can occur in the absence of a receptor-mediated pathway, we transfected COS-7 cells with cDNA encoding recombinant wild-type eNOS or CD8-Myr^-, as above. Cells were then stimulated with the calcium ionophore A23187, which induces eNOS activation and translocation (6). As shown in Fig. 4*B*, recombinant wild-type eNOS in COS-7 cells treated with A23187 (10 μM for 5 min) is denitrosylated (49 ± 12% decrease in *S*-nitrosylation relative to wild-type, $n = 3$, $p < 0.02$). However, as in transfected BAEC, agonist treatment did not affect CD8-Myr^- eNOS *S*-nitrosylation (Fig. 4*B*).

Dynamic S-Nitrosylation of eNOS in Mouse Aorta—To further explore the physiologic relevance of eNOS *S*-nitrosylation, we extended our work from cultured BAEC to intact blood vessels from mice. We first tested whether we could detect *S*-nitrosylation of eNOS immunoprecipitated from preparations of homogenized mouse aorta. As shown in Fig. 5*A*, we were able to detect eNOS and its *S*-nitrosylation in aortic preparations from wild-type mice, but not in aortae from mice in which the eNOS gene had been disrupted. To verify that the signal detected indeed reflects eNOS *S*-nitrosylation, we reacted immunoprecipitated eNOS with $HgCl_2$ before proceeding with the biotin switch method. Hg^{2+} selectively and quantitatively reduces *S*-nitrosothiols (19); as shown in Fig. 5*B*, the *S*-nitrosylation signal of eNOS treated with $HgCl_2$ is almost completely abrogated relative to the control sample. Finally, we tested whether eNOS is dynamically *S*-nitrosylated in intact blood vessels. Intact, freshly harvested aortae were incubated in medium supplemented with VEGF (30 ng/ml) or its vehicle for 5 min before the vessel was homogenized into solution. eNOS was then immunoprecipitated from homogenates prepared from the vessels and processed by the biotin switch method. As shown in Fig. 5*C*, addition of VEGF decreases eNOS *S*-nitrosylation by 82 ± 7% relative to vehicle-treated vessel ($n = 3$, $p < 0.01$ by ANOVA); over this same time period, eNOS phosphorylation at Ser^{1179}, which correlates with VEGF-mediated eNOS activation, is increased (20, 21).

DISCUSSION

We have previously shown that the zinc-tetrathiolate cysteine residues of eNOS (22) are a likely target of functional *S*-nitrosylation, and we have reported that site-directed mutagenesis of the zinc-tetrathiolate cysteines of eNOS to serine abolishes endogenous eNOS *S*-nitrosylation in transfected COS-7 cells (7). In light of data showing that eNOS is reversibly inhibited by *S*-nitrosylation in intact cells, the direct confirmation by MALDI-MS of eNOS *S*-nitrosylation is important for future investigations into the mechanism of this effect (7). Using mass spectrometry, we have confirmed our earlier findings by showing that of the 30 different cysteine residues that are found in the primary sequence of eNOS, only *S*-nitrosylation of a zinc-tetrathiolate residue (Cys^{101}) is detected. This *S*-nitrosothiol was particularly difficult to map because the N terminus of the peptide containing Cys^{101} contains a non-tryptic site, *i.e.* the tryptic peptide containing Cys^{101} should have Cys^{100} as the N-terminal residue. Possible explanations for non-tryptic cleavage of the peptide might be that an excessive quantity of trypsin was used in proteolysis, that non-enzymatic proteolysis of eNOS occurred during the biotin switch assay, or that eNOS $^{99}RCC^{101}$ is predisposed to autoproteolysis. Since several different proteases at various concentrations yielded equivalent results, we suspect that autoproteolysis occurred during the heating and denaturation steps of the biotin switch assay

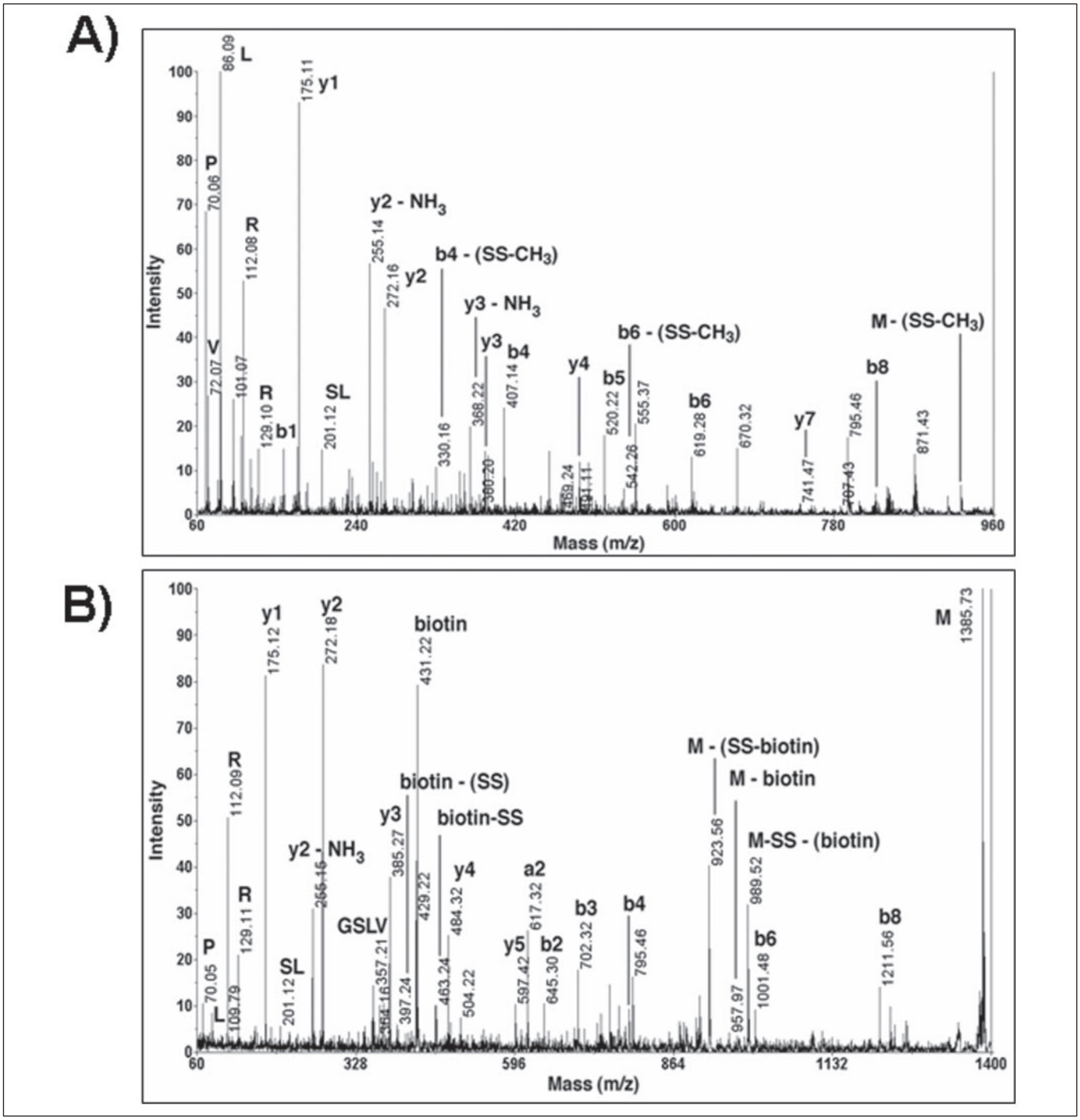

FIGURE 2. **Collision-induced dissociation spectra.** Shown are collision-induced dissociation spectra confirming modification of Cys^{107} by MMTS (*A*) and biotin-HPDP (*B*). For *A*, the CID spectrum of this peptide contains most of the y^+ and b^+ series of ions, an internal amino acid fragment, and peaks corresponding to C-S dissociation of the methyl disulfide. This spectrum confirms the identity of the peptide as the methyl disulfide of CLGSLVLPR. The same disulfide fragmentation pattern (dissociation at C-S) was also observed for b4 and b6. *B* confirms that the C-terminal zinc-tetrathiolate cysteine is the site of biotinylation, indicating that an *S*-nitrosothiol was formed on this amino acid (shown as Cys^{107} in this figure analyzing recombinant eNOS with an N-terminal hexahistidine tag; this residue corresponds to Cys^{101} in the native bovine eNOS). The CID spectrum of this peptide contains most of the y^+ and b^+ series of ions, two internal amino acid fragments, and peaks corresponding to C-S and S-S dissociation of the disulfide-linked biotin. This spectrum confirms the identity of the peptide as *S*-biotinylated CLGSLVLPR. The abbreviations used in this figure include: *M*, molecular ion; *M-SS-(biotin)*, molecular ion minus biotin with the sulfur atom of biotin-HPDP retained (C-S fragmentation); *M-(SS-CH_3)*, molecular ion minus MMTS with the sulfur atom of cysteine released; *M-biotin*, molecular ion minus biotin (S-S fragmentation); *M-(SS-biotin)*, molecular ion minus biotin with the cysteine sulfur atom released (C-S fragmentation). The biotin tags released from these three dissociation events were also observed: biotin-(SS), biotin, and biotin-SS.

(14). Indeed, since arginine is known to be an activator of cysteine-mediated proteolysis, autoproteolysis mediated by an N-S acyl rearrangement during the biotin switch method is plausible (24, 25). Based on our previous studies on the *S*-nitrosylation of the inducible isoform of NO-synthase, we suspect that both cysteines comprising the eNOS zinc-tetrathiolate are *S*-nitrosylated, but the amino acid composition of the peptide containing the C-terminal cysteine precludes efficient desorption/ionization (10). In any instance, we speculate that *S*-nitrosyla-

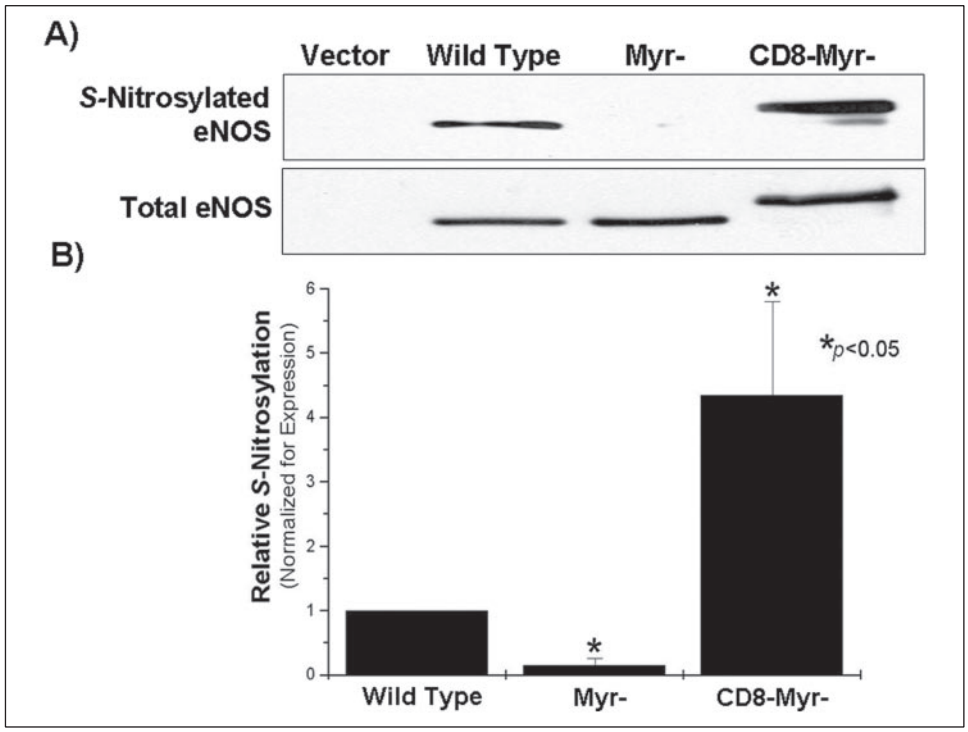

FIGURE 3. **eNOS subcellular targeting and *S*-nitrosylation in transfected COS-7 cells.** Shown are data from three independent experiments that yielded equivalent results from COS-7 cells transfected with cDNA encoding recombinant wild-type eNOS, Myr$^-$ eNOS, or CD8-Myr$^-$ eNOS, as indicated. The recombinant proteins were immunoprecipitated with anti-eNOS antibody from lysates of transfected cells and processed by the biotin switch method, as described under "Experimental Procedures." *S*-Nitrosylation levels of the various recombinant eNOS constructs (*upper blot*) and total starting eNOS levels in cell lysates (*lower blot*) were detected by probing immunoblots with anti-eNOS antibody. Shown in *A* is a representative blot from these experiments. For *B,* densitometric analyses of recombinant eNOS *S*-nitrosylation levels from pooled data were normalized for protein expression and plotted relative to recombinant wild-type eNOS ± S.E. The *asterisk* indicates $p < 0.05$ *versus* wild-type eNOS *S*-nitrosylation levels using ANOVA.

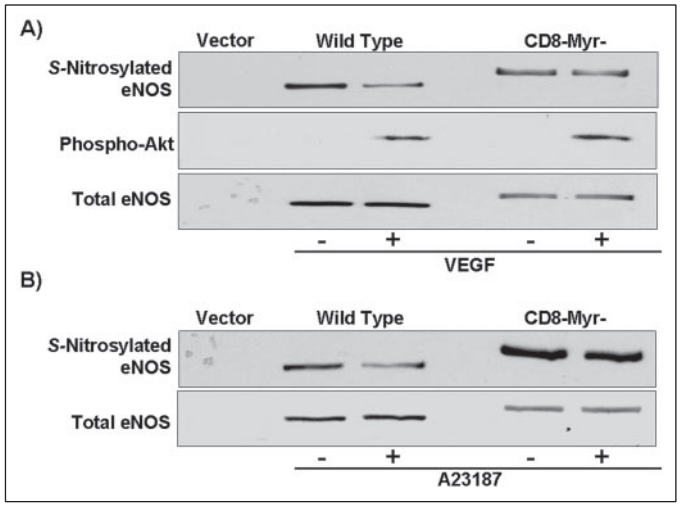

FIGURE 4. **Agonist stimulation and *S*-nitrosylation of wild-type and CD8-Myr$^-$ eNOS in transfected BAEC and COS-7 cells.** Shown in each panel are representative Western blots of eNOS immunoprecipitated from lysates prepared from cells transfected with cDNA encoding recombinant wild-type or CD8-Myr$^-$ eNOS, as indicated. After agonist treatment, recombinant eNOS was immunoprecipitated with either anti-HA-epitope antibody (for *A*) or anti-eNOS antibody (for *B*) and processed by the biotin switch method, as described under "Experimental Procedures." *S*-Nitrosylated eNOS was detected by probing immunoblots with anti-eNOS antibody. Where indicated, phospho-Akt and total recombinant eNOS levels in cell lysates were detected by probing immunoblots with anti-phospho-Akt or anti-HA antibodies, respectively. *A* shows a representative blot of three independent experiments from transfected BAEC treated with VEGF (10 ng/ml for 5 min), or its vehicle, that yielded equivalent results. Shown in *B* is a representative blot of three independent experiments that yielded equivalent results from transfected COS-7 cells treated with A23187 (10 μM for 5 min) or its vehicle.

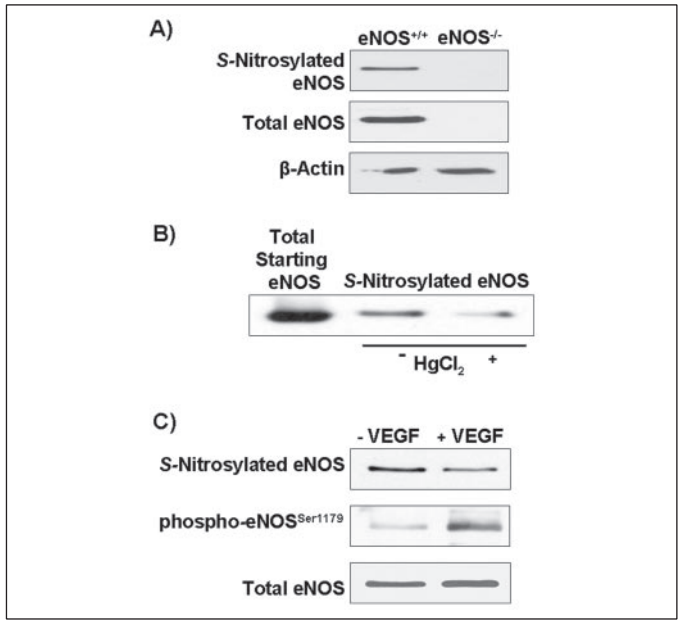

FIGURE 5. **Dynamic agonist-modulated *S*-nitrosylation of eNOS in intact blood vessels.** Shown in *A* is a representative blot from three independent experiments that yielded equivalent results. eNOS was immunoprecipitated from homogenates of aortae derived from wild-type mice (eNOS$^{+/+}$) or mice with a genetic disruption of the eNOS gene (eNOS$^{-/-}$). After processing by the biotin switch method and separation by SDS-PAGE, eNOS *S*-nitrosylation was detected by probing immunoblots with anti-eNOS antibody. Total eNOS and β-actin in starting homogenates were detected by probing immunoblots with antibodies raised against eNOS and β-actin, respectively. Shown in *B* is a representative blot of three independent experiments that yielded equivalent results. Homogenates derived from mouse aorta were separated into two equal fractions. As described under "Experimental Procedures," eNOS was immunoprecipitated with anti-eNOS antibody and reacted with $HgCl_2$ or buffer alone before proceeding with the biotin switch method. After SDS-PAGE, total eNOS and eNOS *S*-nitrosylation were detected by probing immunoblots with anti-eNOS antibody. Shown in *C* is a representative blot of three independent experiments that yielded equivalent results. Freshly prepared aortae were incubated in medium containing VEGF (30 ng/ml) or its vehicle for 5 min before being processed for homogenization, eNOS immunoprecipitation, biotin switch, SDS-PAGE, and anti-eNOS immunoblot, as described under "Experimental Procedures." Total and phosphorylated eNOS from starting homogenates was detected in immunoblots probed with antibodies raised against eNOS or phospho-eNOS-Ser^{1179}, as indicated.

tion of the zinc-tetrathiolate of eNOS induces a change in the quaternary structure of the eNOS dimer that may impair the efficient substrate binding or electron flow between eNOS subunits necessary for maximal enzyme activity (26, 27).

This study also provides evidence that *S*-nitrosylation of eNOS is restricted to membrane-associated eNOS and that translocation of the enzyme to the cytoplasmic compartment is necessary for eNOS deni-

trosylation. As shown in Fig. 3, eNOS *S*-nitrosylation is correlated with targeting to caveolae: Myr$^-$ eNOS, which is restricted to the cytosol (13), is not *S*-nitrosylated, whereas wild-type eNOS, which can reversibly transit between caveolae and internal membrane structures, is robustly *S*-nitrosylated. Importantly, the CD8-Myr$^-$ eNOS, which is irreversibly membrane-associated, is hypernitrosylated relative to wild-type eNOS. Furthermore, our data suggest that translocation between cellular compartments modulates eNOS *S*-nitrosylation. Wild-type eNOS, which undergoes agonist-modulated translocation from peripheral membrane caveolae to internal structures, is denitrosylated upon agonist stimulation (Fig. 4). By contrast, CD8-Myr$^-$, which cannot translocate from caveolae, is not denitrosylated by agonist treatment (Fig. 4). Since CD8-Myr$^-$ is enzymatically active and is agonist-responsive, its failure to undergo agonist-induced denitrosylation probably reflects the irreversible targeting of this eNOS fusion protein to caveolae (3).

Taken together, these data support the hypothesis that cellular membranes, and in this case, caveolae, are privileged subcellular domains that favor the stable formation of protein *S*-nitrosothiols (28–30). This hypothesis is supported by previous studies showing that the reaction of NO and oxygen, which is necessary to form *S*-nitrosylating species (*e.g.* N_2O_3), is greatly enhanced by the higher NO concentration and hydrophobic conditions found in cellular membranes (31, 32). The converse situation may also explain why eNOS within the cytosolic compartment is denitrosylated: the intracellular "reducing" environment, with its high concentrations of reduced thiols such as glutathione and thioredoxin, coupled with the relatively low cytosolic concentrations of NO and the rapid hydrolysis of N_2O_3 in the aqueous cytosol, would promote reduction of protein *S*-nitrosothiols and lead to eNOS denitrosylation (33). Similarly, "housekeeping" enzymes may regulate subcellular concentrations of trans-nitrosylating intermediates to favor protein *S*-nitrosylation or denitrosylation within different subcellular compartments (30, 34, 35). Equally plausible is the hypothesis that eNOS *S*-nitrosylation is determined by membrane- and cytosol-restricted enzymes that directly catalyze changes in eNOS *S*-nitrosylation (36). Under any of these models, our data suggest that segregation of a protein into internal membranes in the cytosol represents a fundamental mechanism of differential *S*-nitrosylation (29).

Dynamic *S*-nitrosylation of eNOS in *ex vivo* preparations of intact blood vessels (Fig. 5) further supports the hypothesis that *S*-nitrosylation is a physiologically relevant regulator of eNOS activity (7). Indeed, it is striking that eNOS is acutely denitrosylated after 5 min of VEGF treatment both in cultured BAEC and in intact aorta. Ongoing studies of eNOS *S*-nitrosylation in tissue preparations will explore further the role of eNOS *S*-nitrosylation under normal and pathologic conditions. Since *S*-nitrosylation is a redox-regulated modification, it is tempting to speculate that the vascular dysfunction associated with conditions of oxidative stress may be related to perturbations in eNOS *S*-nitrosylation (37, 38). The ability to detect eNOS *S*-nitrosylation in a single mouse aorta could facilitate future experimental approaches to study the relationships between eNOS *S*-nitrosylation and systemic diseases such as hypertension and diabetes. NO-dependent signaling in the vascular wall is regulated by complex pathways affecting eNOS subcellular targeting, covalent modifications, and protein-protein interactions (39). Our findings that *S*-nitrosylation, a reversible, redox-mediated regulator of eNOS activity, is determined in part by eNOS subcellular localization may lead to the identification of mechanisms whereby pathophysiological perturbations of eNOS targeting or cellular redox state play a role in regulating eNOS signaling in the vasculature.

REFERENCES

1. Loscalzo, J., and Welch, G. (1995) *Prog. Cardiovasc. Dis.* **38,** 87–104
2. Feron, O., Saldana, F., Michel, J. B., and Michel, T. (1998) *J. Biol. Chem.* **273,** 3125–3128
3. Gonzalez, E., Kou, R., Lin, A. J., Golan, D. E., and Michel, T. (2002) *J. Biol. Chem.* **277,** 39554–39560
4. Shaul, P. W., Smart, E. J., Robinson, L. J., German, Z., Yuhanna, I. S., Ying, Y., Anderson, R. G., and Michel, T. (1996) *J. Biol. Chem.* **271,** 6518–6522
5. Robinson, L. J., Busconi, L., and Michel, T. (1995) *J. Biol. Chem.* **270,** 995–998
6. Prabhakar, P., Thatte, H. S., Goetz, R. M., Cho, M. R., Golan, D. E., and Michel, T. (1998) *J. Biol. Chem.* **273,** 27383–27388
7. Erwin, P. A., Lin, A. J., Golan, D. E., and Michel, T. (2005) *J. Biol. Chem.* **280,** 19888–19894
8. Lamas, S., Marsden, P. A., Li, G. K., Tempst, P., and Michel, T. (1992) *Proc. Natl. Acad. Sci. U. S. A.* **89,** 6348–6352
9. Nishida, C. R., and de Montellano, P. R. O. (1998) *J. Biol. Chem.* **273,** 5566–5571
10. Mitchell, D. A., Erwin, P. A., Michel, T., and Marletta, M. A. (2005) *Biochemistry* **44,** 4636–4647
11. Igarashi, J., Erwin, P. A., Dantas, A. P. V., Chen, H., and Michel, T. (2003) *Proc. Natl. Acad. Sci. U. S. A.* **100,** 10664–10669
12. Igarashi, J., and Michel, T. (2000) *J. Biol. Chem.* **275,** 32363–32370
13. Busconi, L., and Michel, T. (1993) *J. Biol. Chem.* **268,** 8410–8413
14. Jaffrey, S. R., and Snyder, S. H. (2001) *Sci. STKE* **2001,** PL1
15. Jaffrey, S. R., Erdjument-Bromage, H., Ferris, C. D., Tempst, P., and Snyder, S. H. (2001) *Nat. Cell Biol.* **3,** 193–197
16. Kantor, D. B., Lanzrein, M., Stary, S. J., Sandoval, G. M., Smith, W. B., Sullivan, B. M., Davidson, N., and Schuman, E. M. (1996) *Science* **274,** 1744–1748
17. Prabhakar, P., Cheng, V., and Michel, T. (2000) *J. Biol. Chem.* **275,** 19416–19421
18. He, H., Venema, V. J., Gu, X., Venema, R. C., Marrero, M. B., and Caldwell, R. B. (1999) *J. Biol. Chem.* **274,** 25130–25135
19. Mannick, J. B., Hausladen, A., Liu, L., Hess, D. T., Zeng, M., Miao, Q. X., Kane, L. S., Gow, A. J., and Stamler, J. S. (1999) *Science* **284,** 651–654
20. Dimmeler, S., Fleming, I., Fisslthaler, B., Hermann, C., Busse, R., and Zeiher, A. M. (1999) *Nature* **399,** 601–605
21. Fulton, D., Gratton, J. P., McCabe, T. J., Fontana, J., Fujio, Y., Walsh, K., Franke, T. F., Papapetropoulos, A., and Sessa, W. C. (1999) *Nature* **399,** 597–601
22. Raman, C. S., Li, H., Martasek, P., Kral, V., Masters, B. S., and Poulos, T. L. (1998) *Cell* **95,** 939–950
23. Deleted in proof
24. Perler, F. B., Xu, M. Q., and Paulus, H. (1997) *Curr. Opin. Chem. Biol.* **1,** 292–299
25. Paulus, H. (2000) *Annu. Rev. Biochem.* **69,** 447–496
26. Li, H., Raman, C. S., Glaser, C. B., Blasko, E., Young, T. A., Parkinson, J. F., Whitlow, M., and Poulos, T. L. (1999) *J. Biol. Chem.* **274,** 21276–21284
27. Xie, Q. W., Leung, M., Fuortes, M., Sassa, S., and Nathan, C. (1996) *Proc. Natl. Acad. Sci. U. S. A.* **93,** 4891–4896
28. Mannick, J. B., Schonhoff, C., Papeta, N., Ghafourifar, P., Szibor, M., Fang, K., and Gaston, B. (2001) *J. Cell Biol.* **154,** 1111–1116
29. Lancaster, J. R., Jr., and Gaston, B. (2004) *Am. J. Physiol.* **287,** L465–L466
30. Hess, D. T., Matsumoto, A., Kim, S. O., Marshall, H. E., and Stamler, J. S. (2005) *Nat. Rev. Mol. Cell. Biol.* **6,** 150–166
31. Liu, X., Miller, M. J., Joshi, M. S., Thomas, D. D., and Lancaster, J. R., Jr. (1998) *Proc. Natl. Acad. Sci. U. S. A.* **95,** 2175–2179
32. Ravichandran, L. V., Johns, R. A., and Rengasamy, A. (1995) *Am. J. Physiol.* **268,** H2216–H2223
33. Zhang, Y., and Hogg, N. (2004) *Am. J. Physiol.* **287,** L467–L474
34. Liu, L., Hausladen, A., Zeng, M., Que, L., Heitman, J., and Stamler, J. S. (2001) *Nature* **410,** 490–494
35. Sliskovic, I., Raturi, A., and Mutus, B. (2005) *J. Biol. Chem.* **280,** 8733–8741
36. Mitchell, D. A., and Marletta, M. A. (2005) *Nat. Chem. Biol.* **1,** 154–158
37. Stamler, J. S., Lamas, S., and Fang, F. C. (2001) *Cell* **106,** 675–683
38. Ting, H. H., Timimi, F. K., Boles, K. S., Creager, S. J., Ganz, P., and Creager, M. A. (1996) *J. Clin. Invest.* **97,** 22–28
39. Shaul, P. W. (2002) *Annu. Rev. Physiol.* **64,** 749–774